Vein Based Multimodal Biometric System Using Handcrafted and Deep Features

Gurunathan Velliangiri[1], Sudhakar Radhakrishnan[1] and Valentina E Balas[2]

[1]Department of Electronics and Communication Engineering, Dr. Mahalingam College of Engineering and Technology, Pollachi - 642 003, Tamilnadu, India. E- mail: gurunathan@drmcet.ac.in, sudhakar@drmcet.ac.in

[2]Department of Automatics and Applied Software, Aurel Vlaicu University of Arad / Academy of Romanian Scientists, 77 B-dul Revolutiei, 310130 Arad, Romania; E-mail: valentina.balas@uav.ro

Abstract: Vascular biometrics have gained significant attention in recent years due to their superior recognition accuracy compared to traditional biometric modalities. This study introduces a hybrid multimodal vein authentication system that leverages both handcrafted and deep learning-based features extracted from finger and dorsal hand vein images. To capture discriminative texture patterns, Adaptive Log-Gabor and Adaptive Difference of Gaussian filters are applied to both modalities. Simultaneously, deep representations are obtained using advanced convolutional neural network architectures. These diverse features are then combined through both feature-level and score-level fusion techniques to enhance the overall system performance. A set of multiple classifiers is employed to ensure robust identification across various subjects. The proposed framework achieves a high identification accuracy of 98.5% with a corresponding Equal Error Rate (EER) of 0.177, demonstrating its effectiveness in secure biometric authentication applications.

Keywords: vascular biometrics; handcrafted features; deep features; deep learning architectures; feature and score level fusion

1 Introduction

Over the past twenty years, biometric technology has emerged as a leading alternative to conventional authentication methods. In critical fields like military defense and forensic science, ensuring security is paramount. Compared to traditional techniques such as passwords and token-based authentication, biometric systems offer a more reliable and secure means of identity verification [1-4]. These systems rely on identifying individuals using either physical attributes or behavioral patterns. Physical characteristics such as the structure of hand veins, shape of the hand, iris configuration, or facial anatomy are typically

consistent over time. In contrast, behavioral identifiers like walking style, handwriting, typing rhythm, or signals captured from the heart (ECG) and brain (EEG) may fluctuate depending on a person's mood, health, or environment. Due to their consistent nature, physiological biometrics are generally favoured for authentication purposes. Among various biometric techniques, hand vein recognition offers enhanced security due to the internal nature of vein patterns. As these patterns lie beneath the skin, they are naturally shielded from external exposure, making unauthorized replication or acquisition challenging without advanced imaging technology. A remarkable aspect of vein biometrics is their uniqueness even identical twins possess different vein structures [5, 6]. This inherent uniqueness not only improves recognition accuracy but also strengthens data privacy and protection. While single-modality biometric systems are useful, they often face challenges such as limited accuracy and issues with intra- and inter-class variability. To address these shortcomings, multimodal biometric systems have been introduced. These systems combine multiple biometric traits to enhance reliability, reduce error rates, and improve resistance to spoofing. Despite advancements, limited research has been conducted on the fusion of different vein-based modalities such as finger, palm, and dorsal hand veins. Multimodal systems integrate one or more biometric sources and offer superior performance compared to unimodal approaches. In recent years, researchers have explored combining both physiological (e.g., palm prints, fingerprints, hand geometry, ear shapes) and behavioral (e.g., signatures, keystrokes, ECG, EEG) traits to develop more robust authentication frameworks [7-11]. This study proposes a novel multimodal vein recognition system using both finger vein and dorsal hand vein images. The structure of this paper is organized as follows: Section 2 provides an overview of existing literature and recent developments in the field. Section 3 details the methodology adopted for the proposed system. Section 4 discusses the experimental findings and performance evaluation. Finally, Section 5 summarizes the conclusions and suggests avenues for future exploration.

2 Related Work

Lu Yang et al. [12] developed a finger vein-based identification system that concentrates on analyzing specific localized regions rather than the entire finger vein image. They introduced a technique called Locality-Constrained Consistent Dictionary Learning (LCDL) to effectively capture relevant features from these partial segments. This localized strategy enhances the ability of the coding coefficients to differentiate between individuals with greater precision. In another approach, Arya Krishnan et al. [13] proposed a novel method for finger vein recognition by using dynamic vein pulsations. By extracting temporal information from finger vein video recordings, they achieved more accurate segmentation of vein structures. Their system was capable of both recognizing the vein pattern and confirming the user's liveness, yielding a high recognition rate of 96.35% and an

Equal Error Rate (EER) of just 0.8%. To address the limitations of minutiae-based methods in capturing detailed vein structures, Arya Krishnan and Tony Thomas [14] introduced a new vein representation model termed FEBA, which stands for Fork, Eye, Bridge, and Arch. This symbolic representation showed strong resilience to image distortions and provided outstanding performance, with an EER close to 0.02% and an average recognition accuracy of 98%. Khaled Mohamed Alashik and Remzi Yildirim [15] presented a biometric recognition framework using dorsal hand vein patterns supported by Deep Learning and Generative Adversarial Networks (GANs). Their multi-phase feature selection approach efficiently extracted distinctive vein characteristics, achieving an identity recognition rate of 98.36% and maintaining a low error rate of 2.47%. In the domain of feature extraction, Murat Erhan Cimen et al. [16] proposed a fractal-based method specifically designed for dorsal vein analysis. This method involved calculating fractal dimensions across seven angular orientations to capture intricate vein details, enhancing the uniqueness of the extracted features. Focusing on real-time implementation, Mohamed I. Sayed et al. [17] designed a dorsal vein recognition system employing lightweight detection and feature extraction algorithms. The classification stage used the K-nearest neighbors (KNN) algorithm, and experiments demonstrated that the system achieved a reliable performance with an EER of 4.33%. Shuyi Li and Bob Zhang [18] developed a multimodal biometric system incorporating a sparse coding framework. They used sparse binary representations generated via matrix projection to improve recognition across multiple modalities. Their system moved beyond conventional machine learning methods by integrating Deep Learning models, specifically Convolutional Neural Networks (CNNs), to bolster security and recognition accuracy. To further enhance multimodal fusion, Principal Component Analysis (PCA) was refined in their method to better integrate diverse biometric traits such as palmprints, ear shapes, facial features, and finger vein patterns. This improved fusion strategy contributed significantly to the system's overall recognition reliability [19].

3 Proposed System

This paper introduces a vein-based biometric system that combines finger and dorsal vein images for improved authentication. The system architecture, shown in Figure 1, outlines key processing steps. By integrating two vascular traits, it ensures higher accuracy and security than unimodal methods. The following sections explain each stage in detail:

3.1 Preprocessing

In this study, publicly available datasets containing finger vein and dorsal vein images were used, with the captured images exhibiting challenges such as variations in illumination and positioning. To address these issues, a range of image enhancement techniques, including contrast enhancement, image smoothing, histogram equalization, CLAHE, and Modified Speeded-Up Adaptive Contrast Enhancement (MSUACE), were applied [20]. The performance of these techniques was assessed using quality metrics like mean intensity, variance, Peak signal-to-noise ratio (PSNR), structural similarity index (SSIM), and Edge preservation index. CLAHE demonstrated superior performance, effectively enhancing local contrast while maintaining vein structure and minimizing noise, making it the optimal choice for further processing in this study.

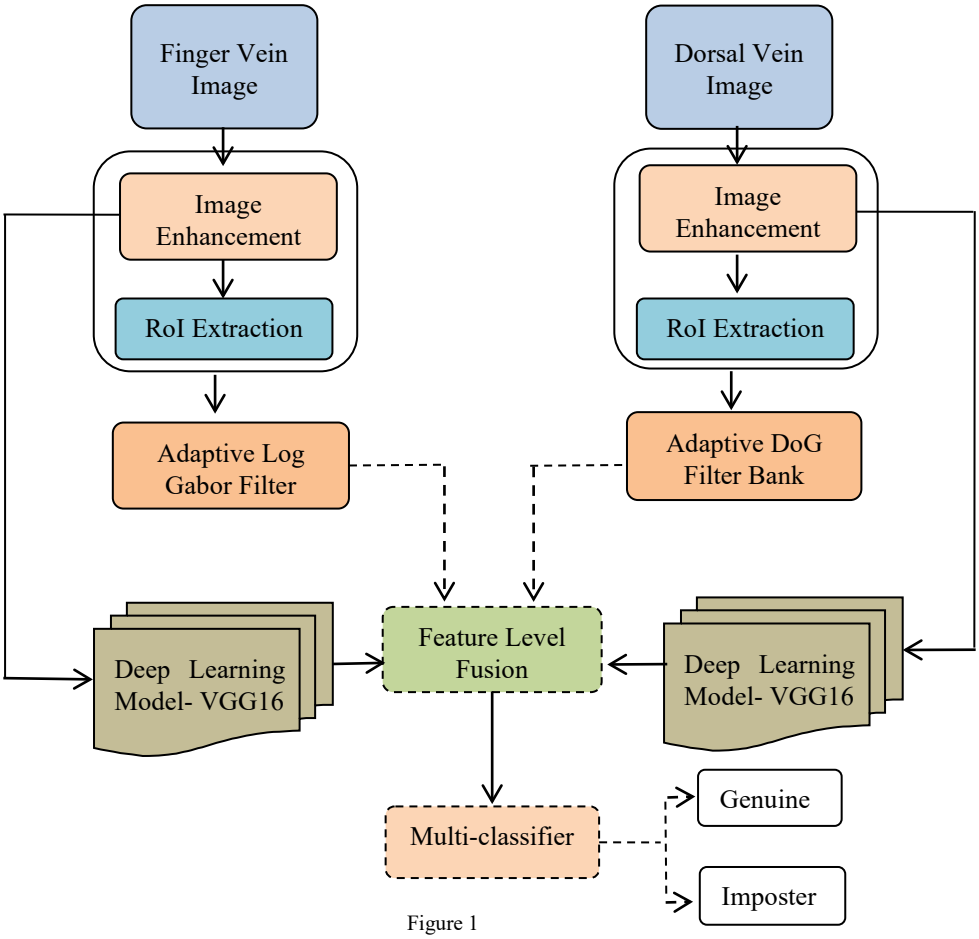

Figure 1
Proposed Multimodal Vein System (Feature level fusion)

3.2 RoI Extraction

Accurate extraction of the vein region faces several challenges, including variations in hand size, inconsistent lighting, different orientations, individual appearance differences, background interference, and uneven gray levels in the foreground. As a result, Region of Interest (RoI) extraction becomes a critical step in hand vein-based biometric system. The vein patterns, being unique to each individual, serve as powerful distinguishing features that help differentiate authorized users from imposters [21].

3.3 Feature Extraction

3.3.1 Adaptive Log-Gabor Filter (ALGF)

To address bandwidth limitations associated with traditional Gabor filters, the Adaptive Log-Gabor Filter (ALGF) is employed for feature extraction from the input images. ALGF is applied at multiple scales and orientations to capture the vein line patterns from the vein images. For the Log-Gabor filter, the scales are set to 4, and the orientations are specified as 6 values ranging from (0º to 180º ({0,π⁄6,π⁄3,π⁄2,2π⁄3,5π⁄6}). To achieve effective feature extraction from vein patterns, the parameters of the Adaptive Log-Gabor Filter (ALGF) were chosen based on extensive empirical analysis [22-24]. The filter was configured with 4 scales and 6 orientations, as this setup offered an optimal balance between feature richness and computational efficiency. Multiple combinations of scales and orientations were tested; this configuration consistently provided the best recognition performance with minimal redundancy. Configurations with higher parameter values led to marginal accuracy improvements but introduced increased feature dimensionality and longer processing time. Based on this analysis, the 4×6 setup was used in all experiments throughout the study. The frequency response of the Log-Gabor filter (LGF) is represented by the equation (1).

$$LGF_{(f_x,\theta_x)}(\rho,\theta) = \exp\left\{-\frac{\left[\log(\frac{\rho}{f_x}\right]^2}{2\sigma_\rho^2}\right\} \times \exp\left\{-\frac{(\theta-\theta_x)^2}{2\sigma_\theta^2}\right\} \quad (1)$$

The polar coordinate system, denoted as (ρ,θ) , the center frequency of LGF is f_x and θ_x indicates the orientation angle relative to LGF. The parameters σ_ρ and σ_θ represents the scale and angular bandwidth. To capture the vein patterns in both finger and dorsal vein images, 40 different ALGF banks were created for feature extraction.

3.3.2 Adaptive Difference of Gaussian (ADoG) Filter

Edge detection using the first-order derivative highlights intensity transitions in an image, enabling the identification of object boundaries and their orientation. However, such gradient-based methods often lack precision in localizing edges and are vulnerable to noise interference. To overcome these limitations, second-order derivative approaches like the Laplacian of Gaussian (LoG) are used, which detect edges by locating zero-crossings in the filtered image. LoG offers improved accuracy in edge localization and enhanced noise robustness [25]. For computational efficiency, the LoG can be effectively approximated using the Difference of Gaussians (DoG). In this work, an Adaptive DoG (ADoG)-based feature extraction framework is employed, and its process flow is represented in Figure 2.

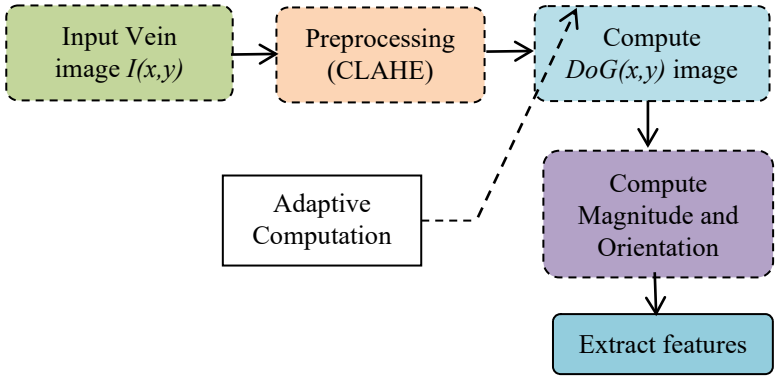

Figure 2
ADoG based feature extraction model

3.3.3 Deep Learning Models

Deep learning techniques are increasingly being adopted in biometric systems to enhance person recognition performance. When working with newly acquired datasets, convolutional neural networks (CNNs) can adapt their parameters effectively especially if trained initially on large-scale datasets. One of the key advantages of deep learning is transfer learning, which addresses the common limitation of having limited training data. A popular method within this framework is fine-tuning, where pre-trained networks such as VGG16 and AlexNet are adapted to a specific task [26, 27]. In the proposed system, deep learning models including VGG16, AlexNet, and GoogleNet are integrated during the recognition phase to improve classification accuracy.

3.4 Feature Fusion

In the proposed approach, fusion is performed at both the feature level and the score level to enhance recognition accuracy. At the feature level, a maximum entropy-based strategy is applied to combine the extracted features effectively. For score-level fusion, a weighted sum rule is used to integrate matching scores from different classifiers. The feature fusion process is illustrated in Figure 3.

The three feature vectors are represented by the equations (2) to (4).

$$f_{ALGF} = \{A_{LGF_1}, A_{LGF_2} \ldots\ldots A_{LGF_N}\} \tag{2}$$

$$f_{ADoG} = \{A_{DoG1}, A_{DoG_2} \ldots\ldots A_{DoG_M}\} \tag{3}$$

$$f_{VGG16} = \{VGG16_1, VGG16_2 \ldots\ldots VGG16_p\} \tag{4}$$

The combined feature vector is represented in Equation (5).

$$Fused\_Feature\_Vector(f) = \sum_{k=1}^{3} \{f_{ALGF\_k}, f_{ADoG\_k}, f_{VGG16\_k}\} \tag{5}$$

The fused feature vector is denoted by f. Entropy-based analysis is applied to the feature vector to identify the most significant features, as shown in Equations (6) and (7).

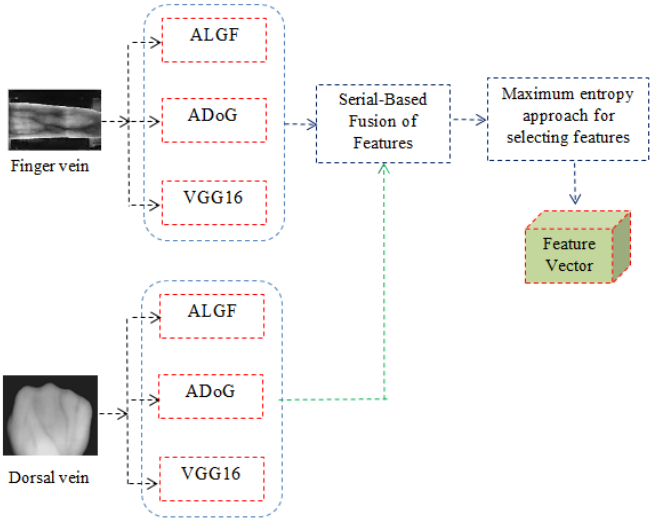

Figure 3
Feature level fusion

The symbol ρ denotes the probability associated with the features and H_e refers to the calculated entropy. Score-level fusion consists of two key phases: normalization and combination. Among the available normalization techniques,

hyperbolic tangent (TanH) normalization offers improved stability and effectiveness. The proposed method uses the weighted sum rule for performing score-level fusion.

$$B_{He} = -NH_{eb} \sum_{i=1}^{n} \rho(f_i) \tag{6}$$

$$f_{optimal\_select} = B_{He}\left(\max\left(f_i\right)\right) \tag{7}$$

3.5 Classification

The proposed system integrates multiple classification algorithms to enhance recognition accuracy in vein biometric analysis. Specifically, Decision Tree (DT), K-Nearest Neighbor (KNN), and Support Vector Machine (SVM) classifiers were employed to evaluate the discriminative capability of the extracted features. These classifiers were selected due to their complementary characteristics in handling complex, high-dimensional feature distributions typical in vein pattern data. SVM, particularly with an RBF kernel, achieved superior results by effectively mapping non-linearly separable data into higher-dimensional spaces, thereby maximizing the margin between classes. KNN was applied for its ability to make predictions based on local proximity, though its performance was influenced by the choice of `k` and distance metric. The Decision Tree classifier, known for its simplicity and interpretability, provided fast classification but exhibited sensitivity to noisy data and a tendency to over-fit. Among the three, SVM consistently delivered the highest classification accuracy, especially in cases with intricate or overlapping vein structures, validating its robustness in biometric recognition tasks [28].

4 Results and Discussion

4.1 Dorsal and Finger vein Dataset

The evaluation of the proposed system was conducted using two publicly available finger vein datasets: SDUMLA-HMT and FV-USM. Additionally, performance testing for dorsal vein recognition was carried out using datasets provided by Felipe Wilches et al. and Dr. Badawi. A detailed overview of all finger and dorsal vein datasets used is presented in Table 1.

Table 1
Summary of the datasets

Attribute/ Datasets	SDUMLA[29]	FV-USM[30]	Felipe Wilches et al[31]	Dr. Badawi hand veins dataset[32]
Subjects	106 (6)	123 (4)	138(4) 113(4)	100(2)
Resolution (pixels)	320 x 240	640 x 480	752 x 560	320 x 240
Image count	3816	2952	1104 678	500

Figure 4 shows sample input images of both finger vein and dorsal vein patterns used in the study.

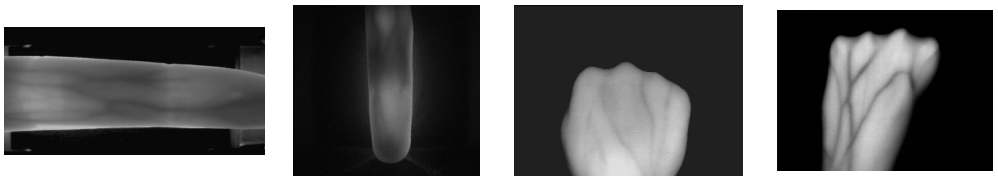

Figure 4
Sample input images of finger vein and dorsal vein patterns

4.2 Preprocessing

Figures 5 and 6 shows the processed images of finger veins and dorsal veins, respectively.

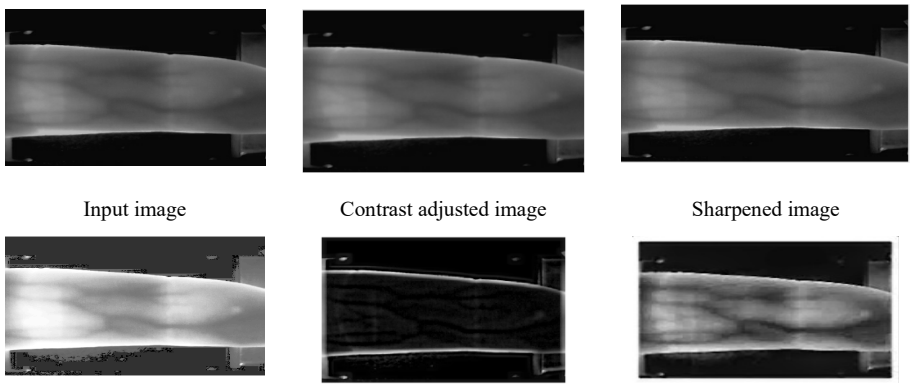

Figure 5
Processed images of finger vein patterns

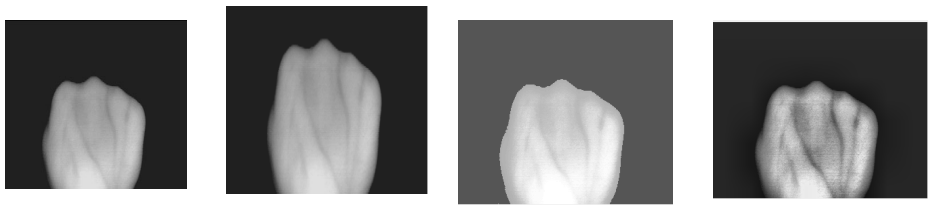

Input image | Sharpened image | Histogram equalized mage | CLAHE image

Figure 6
Enhanced Dorsal vein images

4.3 Feature Extraction

Following the extraction of the Region of Interest (RoI), the vein patterns from the finger images are captured using two distinct filtering techniques: (i) the Adaptive Log-Gabor Filter (ALGF) and (ii) the Adaptive Difference of Gaussian (ADoG) filter bank. The ALGF filter bank contains 40 images, each varied in terms of scale and orientation. For instance, ALGF Design 1 is generated by setting, $f=0.5$, with simultaneous adjustments to both scale and orientation. The results of ALGF design 1 applied to the dorsal and finger vein images are shown in Figure 7. By varying the θ & ρ, multi-directional and multi-scale vein patterns from both finger and dorsal vein are captured for enhanced feature extraction accuracy.

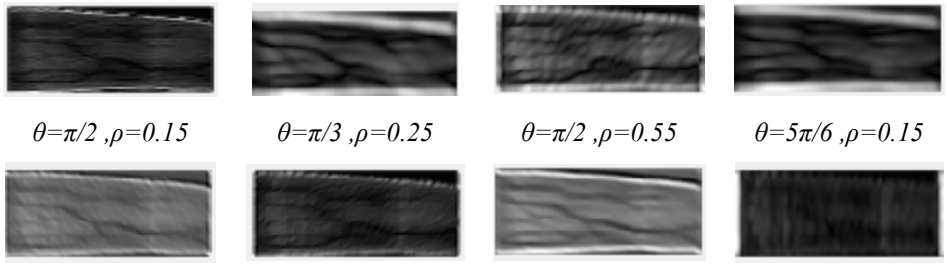

$\theta=\pi/2$,$\rho=0.15$ | $\theta=\pi/3$,$\rho=0.25$ | $\theta=\pi/2$,$\rho=0.55$ | $\theta=5\pi/6$,$\rho=0.15$

$\theta=\pi/6$,$\rho=0.25$ | $\theta=2\pi/3$,$\rho=0.18$ | $\theta=\pi/2$,$\rho=0.27$ | $\theta=\pi/2$,$\rho=0.65$

Figure 7
ALGF-1 ($f = 0.5$) applied to finger vein images at various scales and orientations

As done with the finger vein images, a total of 10 unique ALGF configurations were developed for the dorsal vein dataset. Each design was created by selecting specific frequency values and systematically modifying the scale and orientation settings. For example, the first ALGF configuration was built using a frequency value of $f=0.5$, along with tailored adjustments to scale and orientation. The resulting output of this configuration on dorsal vein images is illustrated in Fig. 8.

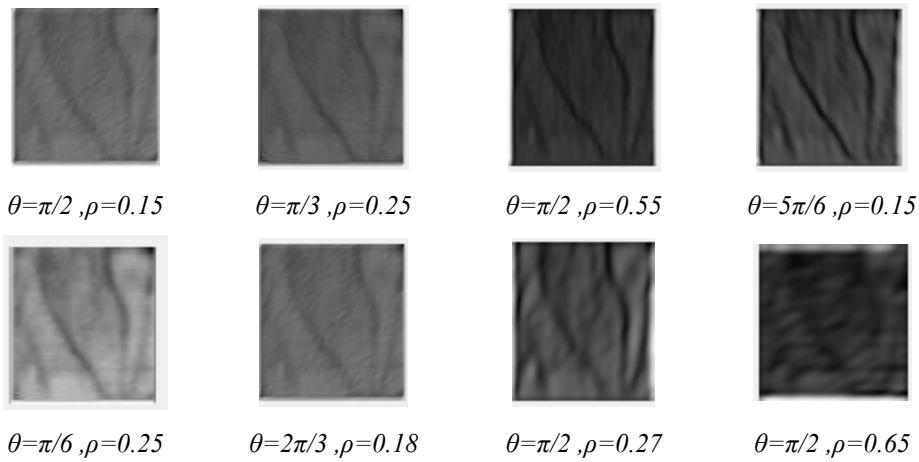

Figure 8

Output of ALGF-1 applied to dorsal vein images with $f=0.5$ across multiple scales and orientations

The proposed biometric authentication system leverages deep learning models such as AlexNet, VGG16, and GoogleNet to extract features from both finger and dorsal vein images. To enhance recognition performance, the system integrates both feature-level and score-level fusion strategies. Its effectiveness is measured using standard evaluation metrics, including Accuracy, Equal Error Rate (EER), False Acceptance Rate (FAR), and False Rejection Rate (FRR).

In this context, a True Positive (TP) indicates the correct recognition of an authorized user, while a False Negative (FN) occurs when a legitimate user is wrongly denied access. A True Negative (TN) refers to the proper rejection of an unauthorized individual, and a False Positive (FP) reflects an incorrect acceptance of an imposter. Specifically, the False Acceptance Rate (FAR) represents the probability that an unauthorized person is mistakenly granted access, as expressed in Equation (8).

$$FAR = \frac{FP}{TN + FP} \tag{8}$$

The False Rejection Rate (FRR) represents the probability that a legitimate user will be mistakenly denied access by the biometric system. This metric is defined in Equation (9).

$$FRR = \frac{FN}{TN + FP} \tag{9}$$

The EER occurs when the False Acceptance Rate (FAR) equals the False Rejection Rate (FRR), representing the optimal balance between false acceptances and false rejections. Figure 9 illustrates the recognition accuracy obtained from unimodal inputs specifically, finger vein and dorsal vein images evaluated on two

different datasets. The experimental analysis shows that applying the ALGF method in conjunction with an SVM classifier results in a recognition accuracy of 95.65% on the SDUMLA finger vein dataset. In comparison, the use of the ADoG method along with the SVM classifier on the Dr. Badawi hand vein dataset achieves an accuracy rate of 90.25%.

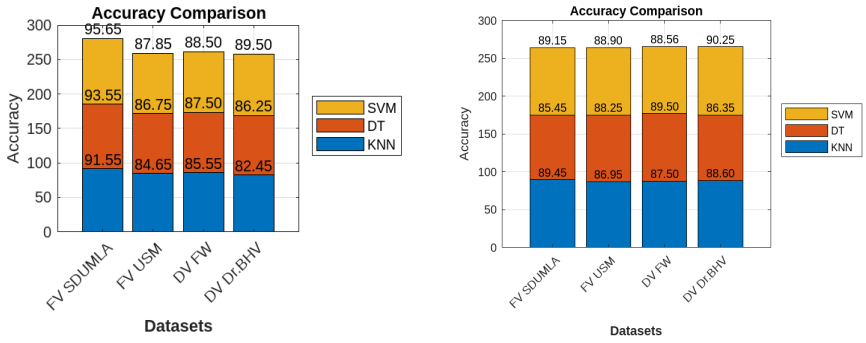

ALGF feature extractor ADoG feature Extractor

Figure 9

Unimodal recognition accuracy for vein images

Table 2 presents the results of applying the VGG16 deep learning model to unimodal biometric modalities. The model achieves an accuracy of 95.65% on the Felipe Wilches finger vein dataset, with an Equal Error Rate (EER) of 1.25%.

Table 2

Performance of VGG16 deep learning architecture

Metric	SDUMLA	FV-USM	Felipe Wilches	Dr. Badawi hand veins dataset
Accuracy (%)	94.25	93.44	**95.65**	95.57
False Acceptance Rate (FAR)	1.98	1.15	**1.28**	1.56
False Rejection Rate (FRR)	2.01	1.76	**1.32**	2.34
Equal Error Rate(EER)	1.65	1.56	**1.25**	1.78

In the proposed multimodal vein authentication system, several fusion approaches were evaluated with different classifiers across four distinct dataset combinations. Table 3 summarizes the accuracy results for the fusion technique, combining ALGF, ADoG, and VGG16, applied to these combinations. The system achieves the highest accuracy of 96.5% when using the SVM classifier.

Figure 10 illustrates the evaluation of the False Acceptance Rate (FAR) and False Rejection Rate (FRR) for various classifiers across different database combinations. The proposed system demonstrates a FAR of 0.95 and an FRR of 0.95 when the SVM classifier is applied to the SDUMLA finger vein and Dr. Badawi hand vein datasets.

Table 3
Accuracy of the Proposed Method across Different Classifiers and Database Combinations

Classifiers	Accuracy of the Proposed Method across Different Classifiers and Database Combinations			
	SDUMLA + Dr. Badawi hand veins	**FV USM + Dr. Badawi hand veins**	**SDUMLA + Felipe Wilches**	**FV USM + Felipe Wilches**
KNN	93.45	94.45	94.5	93.35
DT	94.70	93.65	93.25	92.55
SVM	**96.50**	94.50	96.1	95.75

Table 4 provides a summary of the Equal Error Rate (EER) for the classifiers tested. Using the SVM classifier, the system attains an Equal Error Rate (EER) of 0.95 on both the SDUMLA finger vein and Dr. Badawi hand vein datasets.

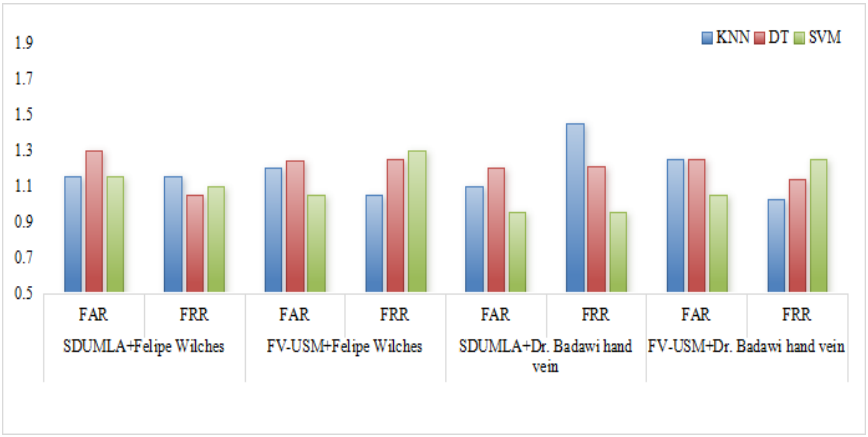

Figure 10
Classifier Performance Analysis: FAR and FRR across Different Dataset Combinations

Table 5 outlines the accuracy results obtained from the proposed approach when employing various deep learning models. Among them, VGG16 delivers the best performance, reaching a top accuracy of 98.5% on the combined SDUMLA finger vein and Dr. Badawi hand vein datasets.

Table 4
Equal Error Rate Analysis for the Proposed System Using Four Dataset Variants

Classifiers	Evaluation of EER for the proposed system with four distinct database combinations			
	SDUMLA + Dr. Badawi hand veins	**FV USM + Dr. Badawi hand veins**	**SDUMLA+ Felipe Wilches**	**FV USM + Felipe Wilches**
KNN	1.275	1.13	1.15	1.125

DT	1.20	1.19	1.18	1.25
SVM	**0.95**	1.15	1.12	1.17

Table 5

Comparative accuracy analysis for different deep learning architectures applied to multiple databases

DL Models	Accuracy (%)			
	SDUMLA + Dr. Badawi hand veins	**FV USM + Dr. Badawi hand veins**	**SDUMLA+ Felipe Wilches**	**FV USM + Felipe Wilches**
VGG16	**98.5**	95.65	96.25	96.56
AlexNet	95.25	95.00	95.65	94.45
GoogleNet	93.00	94.45	94.35	93.45

The higher accuracy achieved by VGG16, compared to AlexNet and GoogleNet, can be attributed to its deeper network architecture and more uniform convolutional layers, which allow for finer-grained feature extraction. The smaller receptive fields in VGG16 help capture detailed spatial patterns in vein images, which are crucial for accurate classification. In contrast, AlexNet and GoogleNet, while effective, may struggle with complex vein textures due to their differing layer configurations and pooling strategies. VGG16's ability to better retain spatial information during feature fusion likely contributed to its higher performance in this study. Figure 11 presents a comparison of the False Acceptance Rate (FAR) and False Rejection Rate (FRR) across different deep learning models. With the VGG16 architecture, the system reports a FAR of 0.105 and an FRR of 0.25 for both the SDUMLA finger vein and Dr. Badawi hand vein datasets. Table 6 provides an overview of the Equal Error Rate (EER) for various deep learning models. The system yields an EER of 0.177 with VGG16 on the SDUMLA finger vein and Dr. Badawi hand vein datasets.

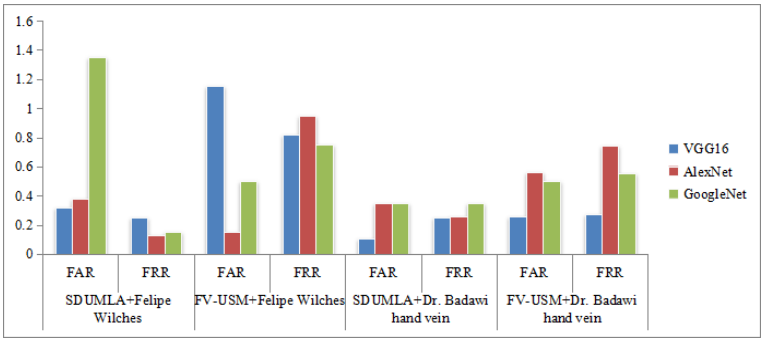

Figure 11

Performance Analysis of Deep Learning Architectures: FAR and FRR across Database Combinations

Table 6
EER performance evaluation for the proposed method using multiple deep learning architectures on diverse databases

DL Models	Assessment of EER across Selected DL Methods			
	SDUMLA + Dr. Badawi hand veins	**FV USM + Dr. Badawi hand veins**	**SDUMLA+ Felipe Wilches**	**FV USM + Felipe Wilches**
VGG16	**0.177**	0.26	0.285	0.985
AlexNet	0.305	0.65	0.25	0.55
GoogleNet	0.35	0.525	0.75	0.625

Table 7 presents the accuracy outcomes of the developed system employing various score-level fusion techniques. Among the evaluated methods, the weighted sum rule demonstrates superior performance, delivering an accuracy of 97.5%. This approach also records a False Acceptance Rate (FAR) of 0.75, a False Rejection Rate (FRR) of 0.95, and an Equal Error Rate (EER) of 0.85 when applied to the combined SDUMLA finger vein and Dr. Badawi hand vein datasets.

Table 7
Comparison of Accuracy across Various Score-Level Fusion Strategies

Fusion scheme	Comparison of Accuracy (%) across Various Score-Level Fusion Strategies			
	SDUMLA + Dr. Badawi hand veins	**FV USM + Dr. Badawi hand veins**	**SDUMLA+ Felipe Wilches**	**FV USM + Felipe Wilches**
Max rule	91.85	90.55	89.45	90.55
Min rule	80.45	78.50	78.65	79.15
Sum rule	92.25	91.25	91.00	91.65
Weighted sum rule	**97.5**	94.45	96.5	93.45

Detailed values of FAR, FRR, and EER for different score-level fusion techniques across various dataset combinations are presented in Tables 8 and 9.

Table 8
Evaluation of FAR and FRR across different score-level fusion techniques for the proposed method

Fusion scheme	Evaluation of FAR and FRR across different score-level fusion scheme							
	SDUMLA + Dr. Badawi hand veins		**FV USM + Dr. Badawi hand veins**		**SDUMLA+ Felipe Wilches**		**FV USM + Felipe Wilches**	
	FAR	**FRR**	**FAR**	**FRR**	**FAR**	**FRR**	**FAR**	**FRR**
Max rule	1.78	1.45	1.35	2.45	2.15	1.64	2.05	1.15
Min rule	2.15	1.95	2.45	3.45	1.75	2.95	1.85	2.65
Sum rule	1.45	0.85	2.15	1.85	1.15	1.35	1.45	1.945
Weighted sum rule	**0.75**	**0.95**	1.05	1.25	0.95	1.25	1.45	1.15

Table 9
Evaluation of EER across different score-level fusion methods in the proposed system

Fusion scheme	Evaluation of EER across different score-level fusion methods			
	SDUMLA + Dr. Badawi hand veins	**FV USM + Dr. Badawi hand veins**	**SDUMLA+ Felipe Wilches**	**FV USM + Felipe Wilches**
Max rule	1.6	1.9	1.89	1.6
Min rule	2.05	2.95	2.35	2.25
Sum rule	1.15	2.0	1.25	1.69
Weighted sum rule	**0.85**	1.15	1.1	1.3

The proposed approach exhibits improved effectiveness when applied to a combination of SDUMLA finger vein and Dr. Badawi hand vein datasets. When using feature-level fusion with the VGG16 model, the system achieves a peak accuracy of 98.5%, along with a False Acceptance Rate (FAR) of 0.105, a False Rejection Rate (FRR) of 0.25, and an Equal Error Rate (EER) of 0.177. In comparison, the use of score-level fusion through the weighted sum strategy results in an accuracy of 97.5%, with FAR, FRR, and EER values recorded at 0.75, 0.95, and 0.85 respectively. Table 10 represents the ablation study of the vein biometric system.

Table 10
Unimodal Accuracy of Finger and Dorsal Veins

Biometric Modality	Dataset	Classifier/ DL model	Accuracy (%)
Finger vein (FV)	FV- SDUMLA	KNN	91.55
		DT	93.55
		SVM	95.65
		VGG16	94.25
		AlexNet	91.24
		GoogleNet	89.12
	FV USM	KNN	84.65
		DT	86.75
		SVM	87.85
		VGG16	93.44
		AlexNet	89.15
		GoogleNet	86.56
Dorsal vein (DV)	DV-FW	KNN	85.55
		DT	87.50
		SVM	88.50
		VGG16	95.65
		AlexNet	86.56
		GoogleNet	87.15

	DV-Dr.BHV	KNN	82.45
		DT	86.25
		SVM	89.50
		VGG16	95.57
		AlexNet	88.12
		GoogleNet	88.10

Table 10 presents the unimodal performance of finger and dorsal vein modalities using traditional classifiers and deep learning models. Among all methods, SVM and VGG16 consistently achieved higher accuracy, indicating their effectiveness in capturing discriminative vein features. The fusion of finger and dorsal vein modalities clearly enhances the performance of the biometric system. The application of feature-level fusion with the VGG16 deep learning architecture, when used on two heterogeneous vascular biometric datasets, produced the maximum recorded recognition accuracy of 98.5%. Score-level fusion using a weighted sum rule also yielded high accuracy across different dataset pairs. Deep learning models, especially VGG16, consistently surpassed traditional classifiers, confirming the strength of multimodal integration in vascular authentication systems as represented in the Table 11. Table 12 compares the proposed method with current leading techniques.

Table 11
Multimodal Accuracy of Finger and Dorsal Veins

Dataset	**Level of fusion**	**Classifier / DL Model**	**Accuracy (%)**
SDUMLA + Dr. Badawi hand veins	Feature level	KNN	93.45
		DT	94.70
		SVM	96.50
		VGG16	**98.5**
		AlexNet	95.25
		Google Net	93.00
	Score level	Weighted sum rule	97.5
FV USM + Dr. Badawi hand veins	Feature level	KNN	94.45
		DT	93.65
		SVM	94.50
		VGG16	95.65
		AlexNet	95.00
		Google Net	94.45
	Score level	Weighted sum rule	94.45
SDUMLA+ Felipe Wilches	Feature level	KNN	94.5
		DT	93.25
		SVM	96.1
		VGG16	96.25

		AlexNet	95.65
		Google Net	94.35
	Score level	Weighted sum rule	96.5
FV USM + Felipe Wilches	Feature level	KNN	93.35
		DT	92.55
		SVM	95.75
		VGG16	96.56
		AlexNet	94.45
		Google Net	93.45
	Score level	Weighted sum rule	93.45

Table 12
Comparative Analysis of Accuracy across Recent Multimodal Biometric Techniques

Author	**Technique/ Approach**	**Modality Used**	**Accuracy**
Shuyi Li et al. [33]	Local discriminant coding with CNN-based feature representation	Fingerprint + Finger vein	77.94%
Ge-Liang Lv et al. [34]	Adaptive radius LBP fusion using a single finger image under NIR setup	Fingerprint + Finger vein	81.39 %
Syed Aqeel Haider et al. [35]	Morphological processing integrated with AlexNet and fuzzy inference system	Hand geometry + Palm vein	92%
Sunusi Bala Abdullahi et al. [36]	Sequence-wise multimodal deep learning using STMFPFV-Net	Fingerprint + Finger vein	>97%
Proposed Method	Fusion of handcrafted (ALGF, ADoG) and deep features using VGG16 with score and feature-level strategies	Finger vein + Dorsal hand vein	98.50

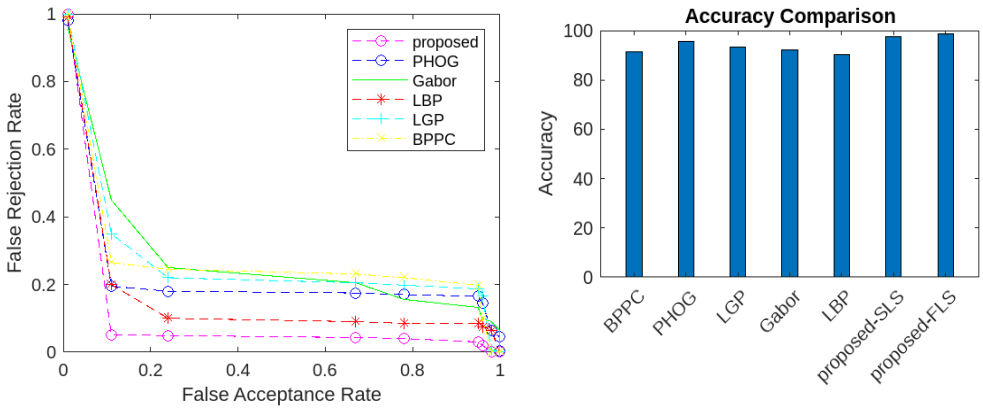

Figure 12
Comparison of recognition accuracy across different feature extraction frameworks

The computational performance of the proposed vascular biometric framework was assessed by recording the execution time for each processing stage. All experiments were carried out in MATLAB 2024a on a workstation configured with an Intel Core i5 (12th Generation) processor, 16 GB of RAM, and an NVIDIA GeForce RTX 3050 GPU. The breakdown of the time consumed by individual stages of the system is presented in Table 13, highlighting the overall computational cost of the approach.

Table 13
Computational time for each stage of the proposed vein biometric recognition systems

Stage	Method used	Computational Time (ms)
Image Enhancement	CLAHE, Histogram Equalization	95
Handcrafted feature extraction	Adaptive Log- Gabor, Adaptive Difference of Gaussian filters	458
Deep Learning - feature extraction	VGG16, AlexNet, Google Net	566
Feature level fusion	Maximum entropy	65
Classification (Classifiers)	DT, KNN and SVM	318
Classification (DL Models)	VGG16, AlexNet, Google Net	874

Conclusion

In this work, a robust multimodal vascular biometric authentication system is presented, incorporating both finger vein and dorsal vein traits. The framework integrates traditional handcrafted feature extraction with modern deep learning approaches, enabling effective use of diverse datasets for improved recognition accuracy. Dual-level fusion strategies were adopted feature-level fusion through the maximum entropy technique and score-level fusion via a weighted summation to enhance performance. Experimental evaluation using the SDUMLA finger vein and Dr. Badawi hand vein datasets demonstrated a maximum accuracy of 96.50% with an SVM classifier. When the VGG16 deep neural network was employed, accuracy improved to 98.5%, while score-level fusion achieved 97.5%. Despite these encouraging results, achieving real-time processing remains a challenge due to the computational demands of deep architectures like VGG16. Consequently, future research will investigate lightweight convolutional models that deliver competitive accuracy with reduced processing requirements. Such models will facilitate faster authentication, making the system more practical for deployment in devices with limited computational capacity.

References

[1] A. K. Jain, A. Ross and S. Prabhakar, “An introduction to biometric recognition”, IEEE Transactions on Circuits and Systems for Video Technology, Vol. 14, No. 1, pp. 4-20, Jan. 2004

[2] Rıdvan Salih Kuzu, Emanuele Maiorana, Patrizio Campisi, “On the intra-subject similarity of hand vein patterns in biometric recognition”, Expert Systems with Applications, Vol. 192, 2022

[3] Kashif Shaheed, Aihua Mao, Imran Qureshi, Munish Kumar, Sumaira Hussain, Xingming Zhang, “Recent advancements in finger vein recognition technology: Methodology, challenges and opportunities”, Information Fusion, Volume 79, pp. 84-109, 2022

[4] A. H. Mohsin et al., "Finger Vein Biometrics: Taxonomy Analysis, Open Challenges, Future Directions, and Recommended Solution for Decentralised Network Architectures," IEEE Access, Vol. 8, pp. 9821-9845, 2020

[5] R. Das, E. Piciucco, E. Maiorana and P. Campisi, "Convolutional Neural Network for Finger-Vein-Based Biometric Identification," IEEE Transactions on Information Forensics and Security, Vol. 14, No. 2, pp. 360-373, 2019

[6] Christof Kauba, Emanuela Piciucco, Emanuele Maiorana, Marta Gomez-Barrero, Bernhard Prommegger, Patrizio Campisi, Andreas Uhl, “Towards practical cancelable biometrics for finger vein recognition”, Information Sciences, Vol. 585, pp. 395-417, 2022

[7] Purohit, H., Ajmera, P. K. “Optimal feature level fusion for secured human authentication in multimodal biometric system”, Machine Vision and Applications, Vol. 32, No. 24, pp. 1-12, 2021

[8] Sahar A, El Rahman, “Multimodal biometric systems based on different fusion levels of ECG and fingerprint using different classifiers”, Soft Computing, Vol. 24, pp. 12599-12632, 2020

[9] Gurjit Singh Walia, Tarandeep Singh, Kuldeep Singh, Neelam Verma, “Robust multimodal biometric system based on optimal score level fusion model”, Expert Systems with Applications, Vol. 116, pp. 364-376, 2019

[10] Bharathi, S, Sudhakar, R and Balas, VE, ‘Hand vein based Multimodal biometric Recognition,’ Acta Polytechnica Hungarica, Vol. 12, No. 6, pp. 213-229, 2015

[11] Bharathi Subramaniam, Sudha V Krishnan, Sudhakar Radhakrishnan and Valentina E Balas, “Fusion of Finger Vein Images, at Score Level, for Personal Authentication”, Acta Polytechnica Hungarica, Vol. 21, No. 6, pp. 53-68, 2024

[12] Lu Yang; Xing Liu, Gongping Yang, Jun Wang; Yilong Yin, “Small-Area Finger Vein Recognition”, IEEE Transactions on Information Forensics and Security, Vol. 18, pp. 1914-1925, 2023

[13] Arya Krishnan, Tony Thomas, Deepak Mishra, “Finger Vein Pulsation-Based Biometric Recognition”, IEEE Transactions on Information Forensics and Security, Vol. 16, pp. 5034-5044, 2021

[14] Arya Krishnan, Tony Thomas, “Finger Vein Recognition Based on Anatomical Features of Vein Patterns”, IEEE Access, Vol. 11, pp. 39373-39384, 2023

[15] Khaled Mohamed Alashik; Remzi Yildirim, “Human Identity Verification From Biometric Dorsal Hand Vein Images Using the DL-GAN Method”, IEEE Access, Vol. 9, pp. 74194-74208, 2021

[16] Murat Erhan Cimen, Omer Faruk Boyraz, Mustafa Zahid Yildiz, Ali Fuat Boz, “A new dorsal hand vein authentication system based on fractal dimension box counting method”, Optik, Vol. 226, No. 1, p. 165438, 2021

[17] Mohamed I. Sayed, Mohamed Taha, Hala H. Zayed, “Real-Time Dorsal Hand Recognition Based on Smartphone”, IEEE Access, Vol. 9, pp. 151118-151128, 2021

[18] Shuyi Li, Bob Zhang, “Joint Discriminative Sparse Coding for Robust Hand-Based Multimodal Recognition”, IEEE Transactions on Information Forensics and Security, Vol. 16, pp. 3186-3198, 2021

[19] Anilkumar Gona and M Subramoniam, “Convolutional neural network with improved feature ranking for robust multi-modal biometric system”, Computers and Electrical Engineering, Vol. 101, p. 108096, 2022

[20] V Gurunathan, S Bharathi, R Sudhakar, “Image enhancement techniques for palm vein images”, IEEE International Conference on Advanced Computing and Communication Systems (ICACCS 2015), Coimbatore, January 2015

[21] Wei Nie, Bob Zhang, “Robust and adaptive ROI extraction for hyperspectral dorsal hand vein images”, IET Computer Vision, Vol. 13, No. 6, pp. 595-604, 2019

[22] Cięszczyk, S, “Application of Gabor, Log-Gabor, and Adaptive Gabor Filters in Determining the Cut-Off Wavelength Shift of TFBG Sensors”, Applied Sciences, Vol. 14, No. 15, pp.1-17, 2024

[23] Xianghai Wang, Zhenhua Mu, Shifu Bai, Ming Wang, Ruoxi Song, Jingzhe Tao & Chuanming Song, “Log-Gabor directional region entropy adaptive guided filtering for multispectral pansharpening”, Applied Intelligence, Vol. 53, pp. 8256-8274, 2023

[24] Wei Wang, Jianwei Li, Feifei Huang, Hailiang Feng, “Design and implementation of Log-Gabor filter in fingerprint image enhancement”, Pattern Recognition Letters, Vol. 29, No. 3, pp. 301-308, 2008

[25] O. Deniz, G. Bueno, J. Salido, and F. De la Torre, "Face recognition using histograms of oriented gradients", Pattern Recognition Letters, Vol. 32, No. 12, pp. 1598-1603, 2011

[26] Chuanqi Tan, Fuchun Sun, Tao Kong, Wenchang Zhang, Chao Yang, Chunfang Liu, "A survey on deep transfer learning", International Conference on Artificial Neural Networks, Greece, pp. 270-279, 2018

[27] Balas. V. E., Roy. S. S., Sharma. D and Samui, P. (Eds.). "Handbook of deep learning applications", Springer, Vol. 136, 2019

[28] S. Li and J. Shawe-Taylor, ''Comparison and fusion of multiresolution features for texture classification,'' Pattern Recognit. Lett., Vol. 26, No. 5, pp. 633-638, Apr. 2005

[29] SDUMLA-HM.: 'Finger vein database', 2016, Available at http:// mla.sdu.edu.cn/info/1006/1195.htmm

[30] Mohd Shahrimie Mohd Asaari, Shahrel A. Suandi, Bakhtiar Affendi Rosdi, "Fusion of Band Limited Phase Only Correlation and Width Centroid Contour Distance for finger based biometrics", Expert Systems with Applications, Vol. 41, No. 7, pp. 3367-3382, 2014

[31] Felipe Wilches-Bernal, Bernardo Núñez-Álvares, Pedro Vizcaya, "A Database of Dorsal Hand Vein Images", https://arxiv.org/abs/2012.05383

[32] Badawi A. M: Hand Vein Database, at Systems and Biomedical Engineering, Cairo University, Cairo, Egypt, 2005

[33] Shuyi Li, Bob Zhang, Shuping Zhao, Jinfeng Yang, "Local discriminant coding based convolutional feature representation for multimodal finger recognition", Information Sciences, Vol. 547, pp. 1170-1181, 2021

[34] Ge-Liang Lv, Lei Shen, Yu-Dong Yao, Hua-Xia Wang, Guo-Dong Zha, "Feature-Level Fusion of Finger Vein and Fingerprint Based on a Single Finger Image: The Use of Incompletely Closed Near-Infrared Equipment", Symmetry, Vol. 12, No. 5, p. 709, 2020

[35] Syed Aqeel Haider, Yawar Rehman, S. M. Usman Ali, "Enhanced Multimodal Biometric Recognition Based upon Intrinsic Hand Biometrics", Electronics, Vol. 9, No. 11, p. 1916, 2020

[36] Sunusi Bala Abdullahi, Zakariyya Abdullahi Bature, Ponlawat Chophuk, Auwal Muhammad, "Sequence-wise multimodal biometric fingerprint and finger-vein recognition network (STMFPFV-Net)", Intelligent Systems with Applications, Vol. 19, p. 200256, 2023